Catalysis Letters (2021) 151:2355–2365
https://doi.org/10.1007/s10562-020-03481-9

Fabrication of Pd–Au Clusters by In Situ Spontaneous Reduction of Reductive Layered Double Hydroxides

Shuai Chen[1] · Haiping Li[1] · Yanan Liu[1,2] · Junting Feng[1,2] · Yufei He[1,2] · Yanfei Wang[3] · Dianqing Li[1,2]

Received: 20 June 2020 / Accepted: 26 November 2020 / Published online: 2 January 2021

Abstract

In this work, layered double hydroxides (LDHs) including the variable valence Co^{2+} ions (CoAl-LDHs) is discovered to be capable of serving as the support and the reducing agent for the fabrication of well-distributed PdAu nanoparticles because of the low potential for reduction. Specifically, the active metal precursors undergo the redox process, in which Co^{2+} is oxidized to Co^{3+}, while active metal ions are successfully reduced to bimetallic PdAu nanoparticles with the dispersion of 73%. Furthermore, the obtained catalysts are evaluated in the selective oxidation of benzyl alcohol as the probing reaction to explore the catalytic behavior. As for intrinsic activity, PdAu/CoAl-LDHs derived by the above in situ spontaneous reduction exhibits activation energy of 62.4 kJ mol^{-1}, much lower than that of PdAu/CoAl-LDHs prepared by sol-immobilization. When the reaction time reaches to 4 h, the benzaldehyde selectivity over the former catalyst is up to 94%, originating from the surface electron starvation of active metals that promotes the hydroxyl groups reacting with O_2 to produce benzaldehyde.

Graphic Abstract

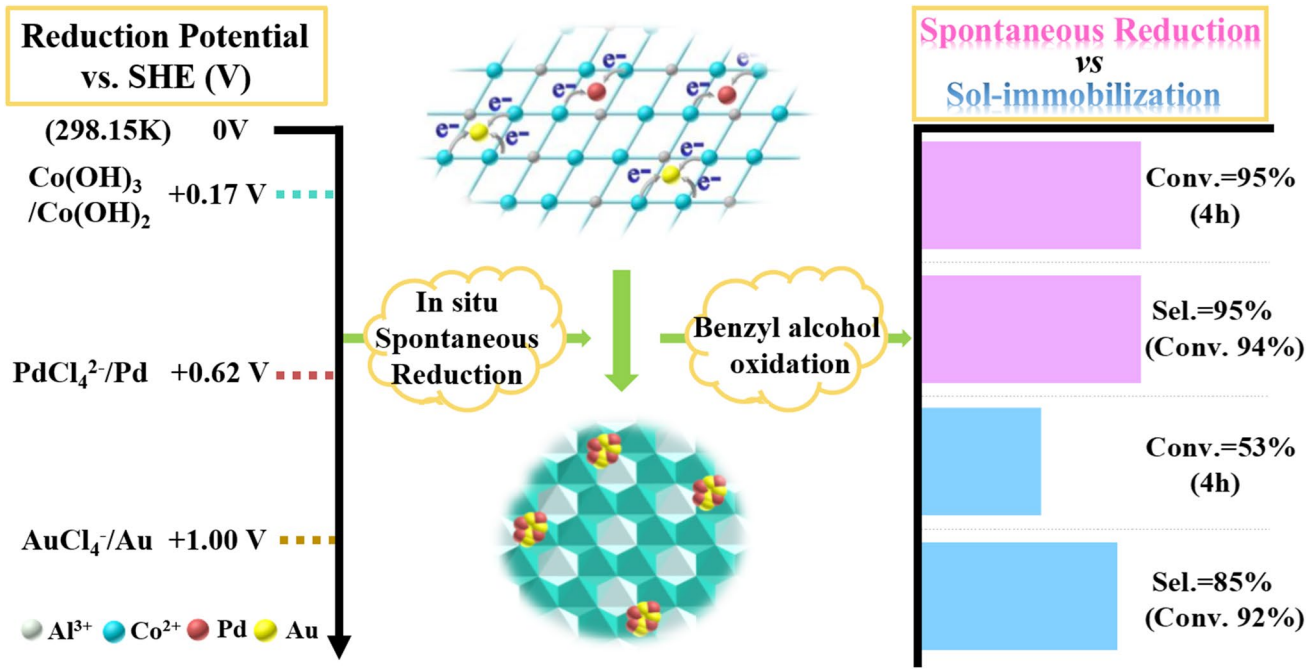

Keywords Spontaneous reduction · Reductive LDHs support · Green preparation · PdAu nanoparticles · Selective oxidation

Extended author information available on the last page of the article

1 Introduction

Supported noble metal catalysts assume enormous importance in the field of petrochemical industry and fine chemical synthesis owing to their preferable catalytic behavior and easy separation, but the scarcity of reserves limits their application [1–3]. Consequently, the demand for developing highly efficient and stable noble metal catalysts with small particle sizes has attracted rapidly increasing attention as the high accessible reactive sites for efficient catalysis [4]. Generally, traditional impregnation has been historically utilized to synthesize catalysts owing to the simple process and low cost, but fail to achieve highly dispersed active metal nanoparticles [5, 6]. In pace with the vigorous development of nanoscience and the deepening of nanotechnology, the researchers created some innovations such as sol immobilization [7], successfully obtaining well-distributed metal catalysts. However, the growing of surface energy as the metal particle size reducing is also apt to result in serious aggregation of metal atoms under weak metal-support interaction, leading to the deactivation [8, 9].

For this above issue, the preferred possible solution for nanometer sized metal catalysts is employing supporting substrate since the catalytic behavior depends strongly on the properties of support materials [10–12]. Dai and his coworker [13] covered electroless deposition of active noble metals on carbon nanotubes through spontaneous redox between metal ions and nanotubes. In this process, the loading of active component on support occurs together with their nucleation. Furthermore, Mao et al. [14] also employed the same method to fabricate Pd nanoparticles with a narrow size distribution (~4 nm) by spontaneous reduction of $PdCl_4^{2-}$ on graphdiyne oxides without the addition of any reducing agent or extra surfactant. The sp^2-hybridized carbon of GO promoted the well and stable dispersion of Pd nanoparticles due to the low potential for reduction and strong interaction with metal atoms. It thus can be concluded that the dispersion degree of the active metal by this method is closely related with the distribution of the reductive site of support. Accordingly, if the distribution of these sites for reduction in the substrate can be effectively controlled, we can further optimize the preparation method to realize an impressive promotion of the dispersion and stability over active metals, and thus improve the efficiency.

Layered double hydroxides (LDHs) are a class of two-dimensional brucite-like inorganic layered materials with the general formula of $[M_{1-x}^{II}M_x^{III}(OH)_2]^{x+}(A^{n-})_{x/n}\cdot mH_2O$ [15–17]. Based on the characteristics of LDHs structure, the M^{II} and M^{III} ions are well-distributed in the atomic level in the laminate [18]. Owing to the flexibility in composition, some of the divalent ions could be replaced by metal ions with a radius similar to that of Mg^{2+} in a wide range of proportion [19]. Inspired by this advantage of LDHs, the variable valence metal ions in low valence state with the reducibility can be introduced into the laminates, and thus achieve the controllable reductive sites in quantity and distribution. This provides the wider opportunity for highly and stably dispersed catalyst derived by the spontaneous in situ reduction method. Recently, our group [20] introduced simultaneously the variable valence transition metal Co and Al into laminate to obtain CoAl-LDHs with good crystallinity, and found that the LDH material including Co^{2+} in the laminate can induce the reduction of active metal Pd. The obtained Pd nanoparticles exhibited the improved metal dispersion (ca. 50%) relative to that obtained by impregnation (ca. 20%) [21], but limited. Additionally, the exploration concerning the influence of different preparation methods on the structure of catalysts in bimetallic system and catalytic performance is still rarely reported.

Herein, in this work, we discover a facile and green route to fabricate CoAl-LDHs supported PdAu nanoparticles by in situ spontaneous redox of support, with the materials derived by sol immobilization as comparison. STEM, XPS and XRD results are exhibited to demonstrate how the precursor of active metal evolves and reduces with the CoAl-LDHs support without the extra reducing agent to yield a highly active and selective catalyst for the oxidation of benzyl alcohol. Detailed characterizations by STEM-mapping, ICP, EDX and XPS give an understanding of how the dispersion and structure of catalysts obtained by different synthesis strategy impacts on catalytic behavior. This work not only offers a novel route to prepare stable and well-dispersed bimetallic catalysts, but also gives an insight into the dependence between the nature of support and active metal.

2 Experimental Section

2.1 Synthesis of CoAl-LDHs

The support was synthesized by a typical co-precipitation method [22, 23]. 5.8210 g of $Co(NO_3)_2\cdot 6H_2O$ and 3.7513 g of $Al(NO_3)_3\cdot 9H_2O$ were dissolved in 100 mL of deionized water with the molar ratio of Co:Al = 2:1 to obtain solution A. 2.1200 g of $NaCO_3$ and 1.9200 g of NaOH were dissolved in 100 mL of deionized water, named solution B. Furthermore, the solution A and B were simultaneously dropped into the flask reactor with the rate of 200 mL h^{-1} at room temperature under vigorous stirring for 6 h. The resulting blue–violet suspension was aged at 90 °C for 4 h, followed by washing with distilled water until pH = 7. The

precipitate was then dried at 90 °C overnight and identified as CoAl-LDHs.

2.2 Preparation of Supported PdAu Catalyst by In Situ Reduction Method

0.5 g of CoAl-LDHs was added to 100 mL of deionized water under vigorous stirring. 165 μL of K_2PdCl_4 solution (50 mM) and 340 μL of $HAuCl_4$ solution (24.3 mM) were then added, and stirred with the speed of 700 rpm for another 6 h at room temperature. The obtained suspension was centrifuged, washed with deionized water until neutral, followed by vacuum freeze-drying for 8 h. The product was denoted as Situ-PdAu/CoAl-LDHs. Similarly, the corresponding monometallic catalysts with same metal loading were also prepared using the above method and named as Situ-Pd/CoAl-LDHs and Situ-Au/CoAl-LDHs, respectively.

2.3 Preparation of Supported PdAu Catalysts by Sol-Immobilization [7]

165 μL of 50 mM K_2PdCl_4 solution and 340 μL of 24.3 mM $HAuCl_4$ solution together with 3.12 mg of $NaBH_4$ and 3.00 mg of PVA were mixed together under vigorous stirring, in which polyvinylpyrrolidone (PVP) was used as a stabilizer, and sodium borohydride ($NaBH_4$) as a reducing agent. After stirring for 1 h, grey PdAu colloidal solution was obtained. 0.50 g of CoAl-LDHs was then poured into above colloidal solution and stirred at room temperature for another 2 h. The resulting suspension was centrifuged, washed with deionized water, and dried in the vacuum at − 50 °C freeze-drying for 8 h. The product was denoted as Sol-PdAu/CoAl-LDHs.

2.4 Characterization

The crystal structures of CoAl-LDHs and catalysts were characterized by X-ray diffraction (XRD) using Shimadzu XRD-600 with Cu Kα (λ = 0.154 nm) as a radiation source with a rate of 10° min^{-1} from 3° to 70°. The morphology of support was characterized by scanning electron microscopy (SEM, JEM-ARM 200F) equipped with an energy dispersive spectrometer (EDS). JEOL JEM-2100F high-resolution transmission electron microscopy (HRTEM) and a high-angle annular dark-fifield scanning transmission electron microscopy (HAADF-STEM) were employed to collect the particle size and structure of catalysts. The electronic structure was obtained by X-ray photoelectron spectroscopy (XPS) using Thermo VG ESCALAB 250 spectrometer with Al Kα anode as the source. The calibration peak was the C 1s peak at 284.6 eV. The compositions were determined by inductively coupled plasma emission spectroscopy (ICP-AES) using an ICP AES-6300.

2.5 The Testing of Benzyl Alcohol Oxidation

The performance of the catalysts was evaluated using a parallel reactor with 50 mL of reaction flask. Prior to the reaction, the air in the reaction flask was drained by filling oxygen. Then, 87.6 mg of catalyst, 5 mL of toluene (solvent) and 3 mL of benzyl alcohol were added with 0.1 MPa O_2, in which the molar ratio of benzyl alcohol to the sum of Pd and Au (Pd/Au molar ratio is calculated as 1) is 10,000:1. The reactor was preheated to 100 °C with a high speed of 900 rpm. After each 1 h, the reaction was stopped and the resulting mixture was cooled to room temperature in an ice bath and collected by filtration. Finally, 0.5 mL of the products mixing with 0.5 mL of mesitylene as internal standard were investigated by gas chromatography (Agilent J&W) equipped with an FID detector and a DB-WAX capillary column (30 m × 0.320 mm, df = 0.25 μm). The kinetic study of the prepared supported bimetallic catalysts was carried out by controlling the appropriate reaction time to make sure that the conversion was lower than 15%. The reaction temperature was changed from 90 to 105 °C but maintained other reaction conditions in agreement with testing of catalytic performance.

3 Results and Discussion

3.1 Characterization of the Catalysts

To investigate the crystal structure, XRD analysis of CoAl-LDHs support and the prepared catalysts by different method were performed. The patterns of CoAl-LDH in Fig. 1a exhibit the typical (003), (006), (009) and (110) reflections with excellent symmetry at $2\theta \approx 12.2°$, 24.5°, 33.5° and 59.7°, which is roughly in agreement with LDHs materials (JCPDS No. 37-0630), indicating CoAl-LDHs with good crystallinity are successfully synthesized [24]. Based on the diffraction position of (003) facet ($2\theta = 11.6°$), it is calculated that the basal spacing of CoAl-LDHs is 0.722 nm, illustrating that the anion in interlayer is CO_3^{2-} [25]. The SEM images shown in Fig. 1b reveals that CoAl-LDH displays a layered hexagonal structure of typical LDHs with particle size of ca. two hundreds of nanometers. Furthermore, the corresponding EDS measurements were also carried out to detect the element distributions and contents. As expected, the data demonstrate that Co/Al atomic mole ratios in CoAl-LDH (2.2) roughly correspond to mole portion of each precursor (2.0), and the distributions of Al, Co and O elements in the layers of LDHs are very uniform.

In principle, in the process of LDH inducing reduction of metal ions, the change of Gibbs free energy (ΔG^{θ}) of redox reaction under standard condition should be less than 0. Meanwhile, ΔG^{θ} is directly related to the standard

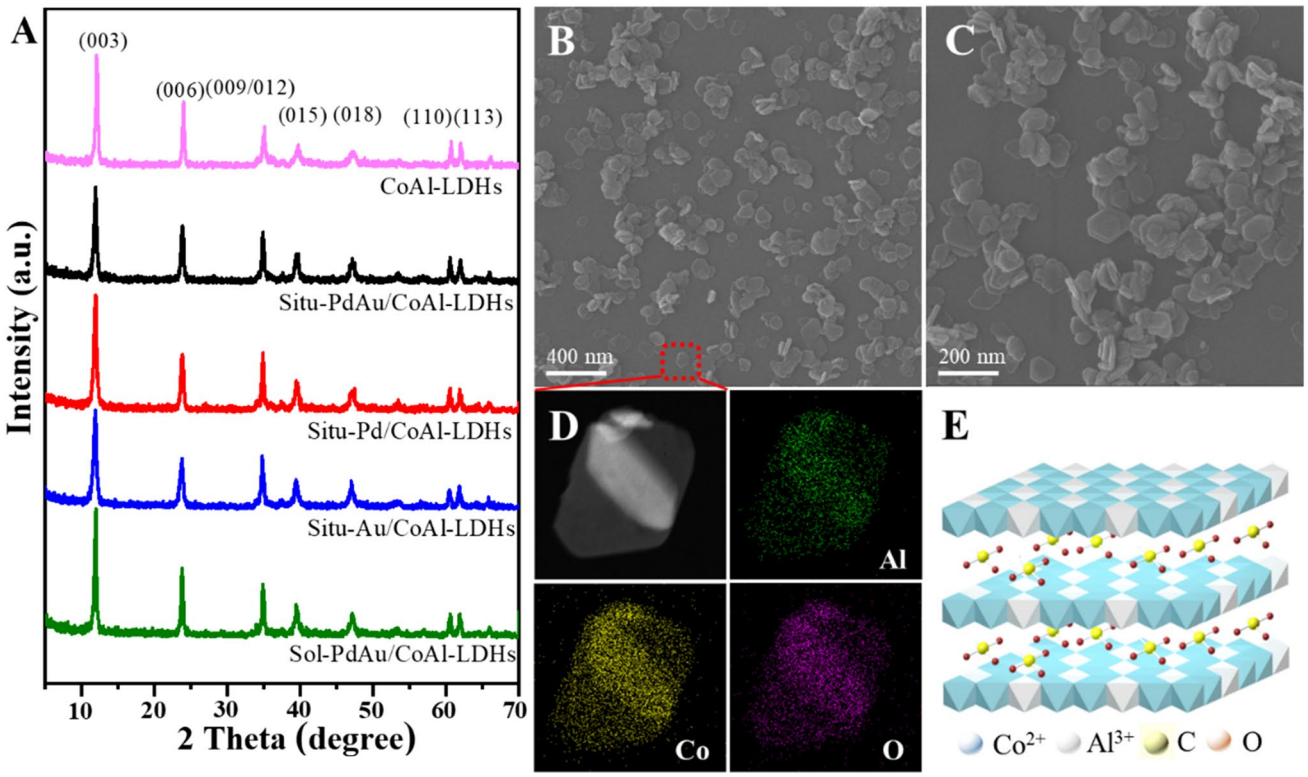

Fig. 1 **a** XRD patterns of support and catalysts. **b**, **c** SEM image of CoAl-LDHs. **d** EDS mapping of Al, Co and O elements in CoAl-LDHs. **e** Model structure diagram of CoAl-LDHs

electromotive force (E^{θ}) of electron pair involved in the reaction [26, 27]. When E^{θ} is greater than 0, LDH inducing reduction of metals can occur spontaneously in thermodynamics. Consequently in this work, the prepared CoAl-LDHs are employed as not only the support but also the reducing agent to fabricate catalyst due to the low reduction potential, with the samples derived from sol-immobilization for comparison. XRD results show that the number and position of peaks of PdAu catalysts (Fig. 1a) present no obvious change after loading Pd and Au relative to pristine CoAl-LDHs, regardless of the preparation method. Three points can be focused on this data. Firstly, CoAl-LDHs possesses excellent stability during the process of the catalyst preparation. Secondly, the absence of characteristic diffraction peaks of Au and Pd elements may be due to the detection limit of instrument or high dispersion of active metal on the catalyst surface. Thirdly, relative to pristine support, the diffraction peak of catalysts exhibits a slight shift to higher angle, indicating that the deformation of MO_6 octahedron in laminate [28, 29]. Based on the octahedral deformation criterion of LDHs, this phenomenon could be originated from the interaction of active metal precursor and reductive support rather than the entering of the former into laminate owing to their large atom radius [30].

To further explore the distribution of active metal atoms, HRTEM measurement was carried out. As expected, the corresponding images of PdAu catalysts (Figs. 2, 3) show that PdAu nanoparticles obtained by in situ reduction method disperse more homogeneously relative to those by sol-immobilization. To survey the size distribution, more than 200 metal particles are randomly selected. Situ-PdAu/CoAl-LDHs catalyst displays a narrow size distribution from 0.8 to 1.7 nm with the mean size of PdAu particles is 1.2 ± 0.3 nm (Fig. 2a), much smaller than that of Sol-PdAu/CoAl-LDHs (3.0 ± 0.8 nm), displayed in Fig. 3a. The metal dispersions of these two PdAu catalysts are further calculated using the mean size derived from HRTEM analysis by assuming the metal particles to be spherical based on the following equation [31]:

$$D = \frac{6A}{\rho \sigma L d}$$

where A is atomic mass, ρ is the density, σ is the average surface area occupied by one active metal atom, L is the Avogadro's constant. It is significantly observed that the metal dispersion of Situ-PdAu/CoAl-LDHs (73%) is more than twofold higher than that of Sol-PdAu/CoAl-LDHs (31%).

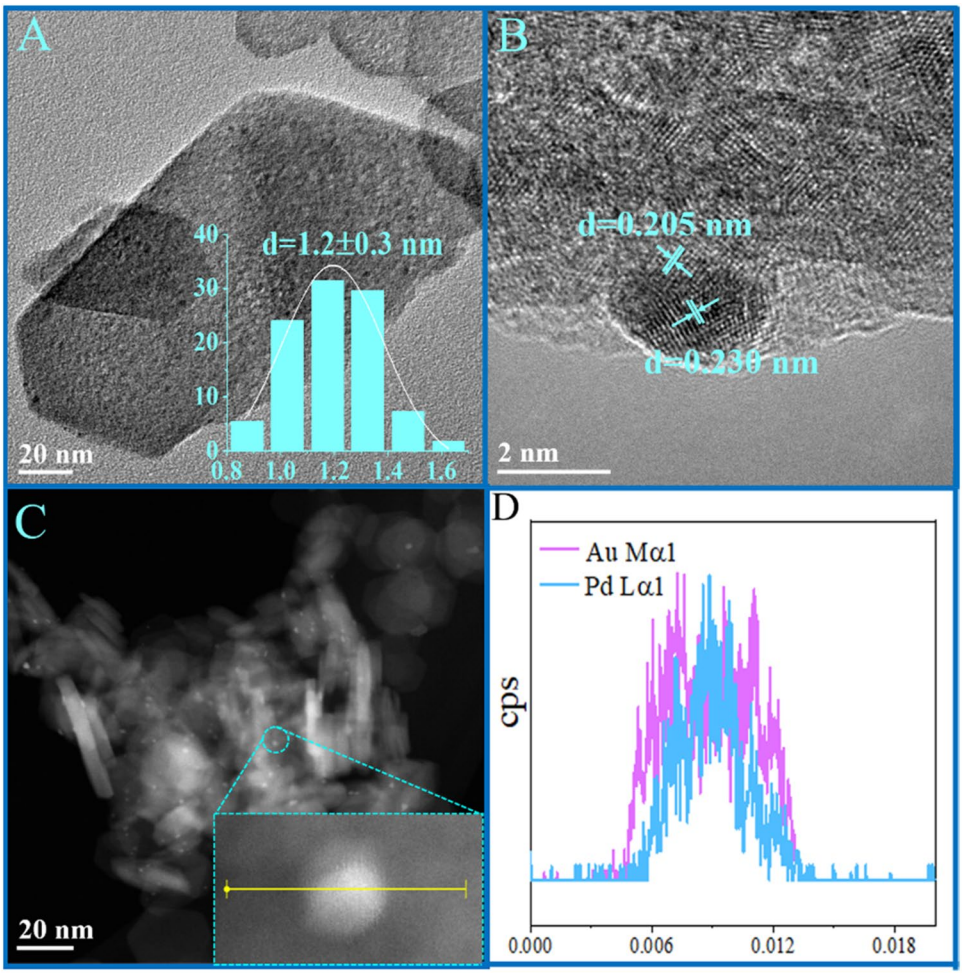

Fig. 2 HRTEM images of Situ-PdAu/CoAl-LDHs

Moreover, HAADF-STEM measurement was also performed, and the images (Figs. 2b, 3b) display the lattice distance of the observed nanoparticles discerning with 0.230 and 0.205 nm, indexed to the planes in PdAu alloy and monometallic Au, respectively [32]. This proves that the reductive site in LDHs can induce the reduction of active metal ions during the process of support spontaneous in situ redox. In addition, the mapping elemental scanning shows that the outer layer of the PdAu nanoparticle is rich in Au, while the intermediate layer is composed of Pd and Au, indicating the formation of Au surface enriched PdAu alloy structure [33].

3.2 Electronic Effect of the Catalysts

To clarify the electronic interaction of metal-support and Pd–Au in this series of samples, XPS analysis was employed, and the results are shown in Fig. 4 and Table 1. Figure 4 illustrates that the core lines of Co 2p are split into two peaks, in which the lower one appears the electron transitions of Co $2p_{1/2}$, and the one at higher binding energy (BE) is originated from the electron transitions of Co $2p_{3/2}$. Furthermore, the spectra in the Co $2p_{3/2}$ region are deconvoluted into three peaks, corresponding to Co^{3+} (780.9 eV), Co^{2+} (782.4 eV) and satellite peaks attributed to Co^{2+} in a high spin state (786.1 eV), respectively [34, 35]. The absence of peaks corresponding to Co^0 demonstrates that all the Co^{2+} precursors have been not reduced. Notably, after introducing the metal precursors, the main peaks in Co 2p3/2 and Co 2p1/2 shift to higher energy (0.2–0.8 eV). Meanwhile, the ratio of Co^{2+} to Co^{3+} in the catalysts decreases relative to that of pristine CoAl-LDHs, meaning that part of Co^{2+} loses electrons to transform into Co^{3+} during the preparation process of the catalysts.

Similarly, XPS spectra of catalysts within the region of Au $4f_{7/2}$ and Pd $3d_{5/2}$ (Fig. 5a, b) also contains two main peaks, corresponding to the characteristic peaks of $M^{\delta+}$ and M^0 ($M^{\delta+} = Au^+$ and Pd^{2+}, $M^0 = Au^0$ and Pd^0) [36, 37], although Pd $3d_{5/2}$ partially overlaps with Au $4d_{5/2}$ in Fig. 5b. The presence of Au^0 and Pd^0 in the catalyst prepared by in-situ reduction method proves that the noble metal ions could capture the lost electrons from Co^{2+}, and then are effectively reduced although without additional reducing agent. Combining with XPS results of Co, it can be concluded that the redox reaction, as shown in Eqs. (1) and (2), indeed occurs

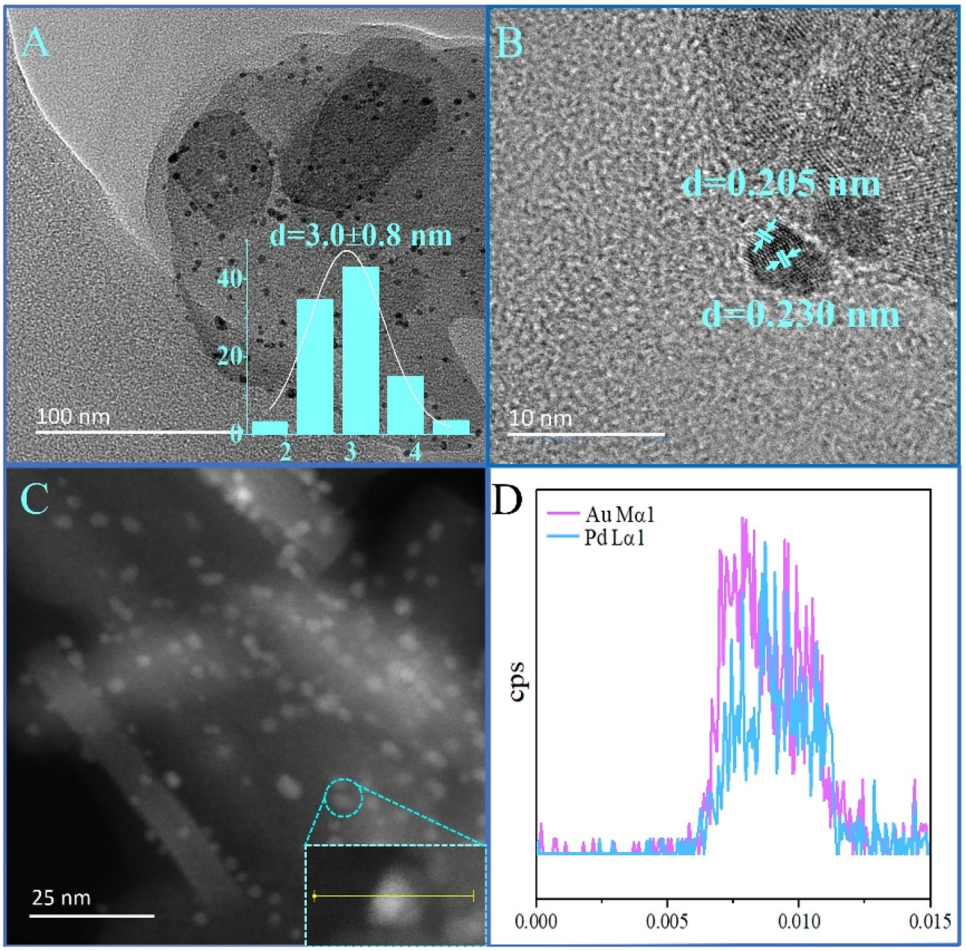

Fig. 3 HRTEM images of Sol-PdAu/CoAl-LDHs

in the preparation process of catalyst, consistent with the results obtained by HRTEM. However, part of oxidized Au^{+} and Pd^{2+} are also observed, which may be due to the re-oxidation in the air. The Au^{0}/Au^{+} and Pd^{0}/Pd^{2+} ratios of catalysts are further calculated, listed in Table 1. Notably, Au^{0}/Au^{+} ratio in Situ-PdAu/CoAl-LDHs (0.7) is basically similar to that of monometallic Situ-Au catalyst (0.9), while Pd^{0}/Pd^{2+} ratio of Situ-PdAu/CoAl-LDHs (1.8) is much higher than that of monometallic Pd sample (0.7). Combined with the conclusion from STEM-EDX analysis, this result indicates that Au enriched on the surface of bimetallic PdAu tends to be in the oxidation states than Pd enriched in the interior in the storage or characterization process.

$$3Co^{2+} + AuCl_4^- \rightarrow 3Co^{3+} + Au + 4Cl^- \quad (1)$$

$$2Co^{2+} + PdCl_4^{2-} \rightarrow 2Co^{3+} + Pd + 4Cl^- \quad (2)$$

Furthermore, the Pd $3d_{5/2}$ and Pd $3d_{3/2}$ peaks assigned to Pd^{0} of Situ-PdAu/CoAl-LDHs shift to higher BE by ca. 0.4 eV compared with the monometallic Pd catalyst (Fig. 5b, Table 1), indicating a decrease in the electron density of Pd in these two catalysts. As expected, negative shifts over the peaks ascribed to metallic Au in these two samples are observed. The decrease in BE of Au and the increase in BE of Pd over bimetallic catalysts could be responsible for the charge transfer from Pd to Au [38]. It is noteworthy that the shifts for the peak corresponding to Pd in Situ-PdAu/CoAl-LDHs are significantly higher (336.9 eV) than those in Sol-PdAu/CoAl-LDHs (335.1 eV), meaning that the active metal in Situ-PdAu/CoAl-LDHs are more electron-deficient. In the previous work, Qi and Zhao et al. [14, 37] discovered the similar high BE value of Pd^{0} in Pd based catalyst prepared by electroless deposition and self-redox method, originating from the preparation method and the interaction between the as-formed Pd nanoparticles and support. This also accounts for the unusual phenomenon in our situation. Additionally, the surface elemental composition of the materials was further determined by XPS (Table 2). The Pd/Au molar ratios in the surface of Situ-PdAu/CoAl-LDHs and Sol-PdAu/CoAl-LDHs are 0.7 and 0.5, while the ratio in the bulk measured by STEM-EDS are 1.2 and 1.1, respectively. It indicates that Au is enriched on the surface, while the intermediate layer is composed of Pd and Au, which is in agreement with the results of STEM-mapping.

Based on the above results, a possible mechanism of catalysts support inducing the reduction of the active metal is proposed in Scheme 1. Initially, the spontaneous in situ redox reaction occurs between the precursor of active metal and the variable valance Co sites in the support, where active metal ions including Pd^{2+} and Au^{3+} are reduced to Pd^0 and Au^0, while Co^{2+} is oxidized to Co^{3+}. Meanwhile, the left Co^{2+} ions could serve as the sites to anchor the reduced metal nanoparticles through the metal-support interaction, contributing that high dispersion of active metal. After the loading, the CoAl-LDHs support is observed to be stable.

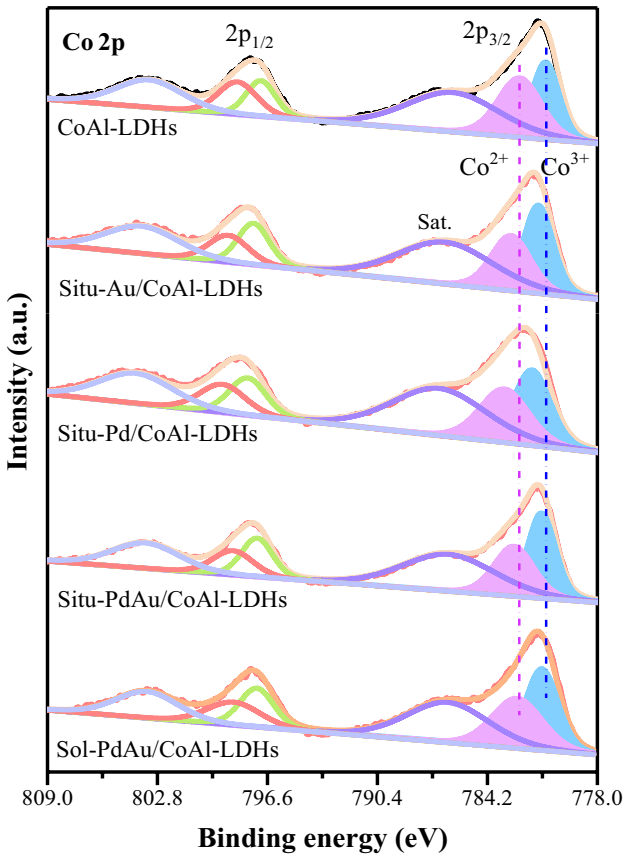

Fig. 4 XPS spectra of Co 2p over the catalysts

3.3 Catalytic Activity Over Selective Oxidation of Benzyl Alcohol

The selective oxidation of benzyl alcohol was employed to evaluate the catalytic behavior including the activity and selectivity of Situ-PdAu/CoAl-LDHs catalysts, with bimetallic Sol-PdAu/CoAl-LDHs and monometallic Pd as well as Au catalysts as control samples. The loading of active metal in catalysts, obtained from ICP analysis, are shown in Table 2. The experimental values of catalysts are slightly lower than theoretical value, but the values are reproducible. Figure 6a exhibits the conversion of benzyl alcohol over these catalysts versus reaction time. It is clearly illustrated that the conversion of bimetallic PdAu catalyst prepared by the spontaneous in situ redox method is higher than that of Sol-PdAu/CoAl-LDHs at any fixed reaction time. When the time raised to 4 h, the conversion of benzyl alcohol over Situ-PdAu/CoAl-LDHs reached 95%, two times higher than that of Sol-PdAu/CoAl-LDHs sample (50%). Turnover frequency (TOF) as an important metric to estimate the intrinsic activity was evaluated at the conversion less than 15%, excluding the effect of mass transfer and heat transfer. The calculation formula is as follow.

$$\mathrm{TOF}\left(\mathrm{h}^{-1}\right) = \frac{\mathrm{n}_{(\text{Benzyl alcohol})}(\mathrm{mol}) \times \text{conversion}}{\frac{\mathrm{m}_{\mathrm{cat}}(\mathrm{g}) \times w\%}{\mathrm{M}_{\overline{\mathrm{PdAu}}}\left(\mathrm{g\ mol}^{-1}\right)} \times \mathrm{t(h)} \times \mathrm{D}}$$

Situ-PdAu/CoAl-LDH exhibits 4270 h^{-1} of TOF, two times higher than that of Sol-PdAu/CoAl-LDHs (2220 h^{-1}). These results demonstrate that PdAu catalyst prepared by the spontaneous in situ reduction method are highly active, which is ascribed to improved dispersion, exposing more active sites for the oxidation of benzyl alcohol [39, 40]. Moreover, the apparent activation energy (Ea), as a vital metric to assess the intrinsic activity, was further investigated. In this study, E_a is obtained from the slope of lnk plotted as a function of T^{-1} under low conversion (< 15%) to rule out the effect of the mass or heat transfer [41, 42] (Fig. 7). The fitting accuracy for each case suggests that the data are reliable. E_a value of Situ-PdAu/CoAl-LDHs is 62.4 kJ mol^{-1}, comparable to

Table 1 Chemical states and binding energy of Co, Au and Pd in samples

Samples	Co^{2+}/Co^{3+}	Au^0/Au^+	Pd^0/Pd^{2+}	Binding energy (eV)			
				$Au^0\ 4f_{7/2}$	$Au^+\ 4f_{7/2}$	$Pd^0\ 3d_{5/2}$	$Pd^{2+}\ 3d_{5/2}$
CoAl-LDHs	1.2	–	–	–	–	–	–
Situ-Au/CoAl-LDHs	0.8	0.9	–	83.7	84.8	–	–
Situ-Pd/CoAl-LDHs	0.9	–	0.7	–	–	336.9	338.6
Situ-PdAu/CoAl-LDHs	0.8	0.7	1.8	83.5	84.6	337.3	338.2
Sol-PdAu/CoAl-LDHs	0.9	0.7	1.0	82.2	83.3	335.1	336.3

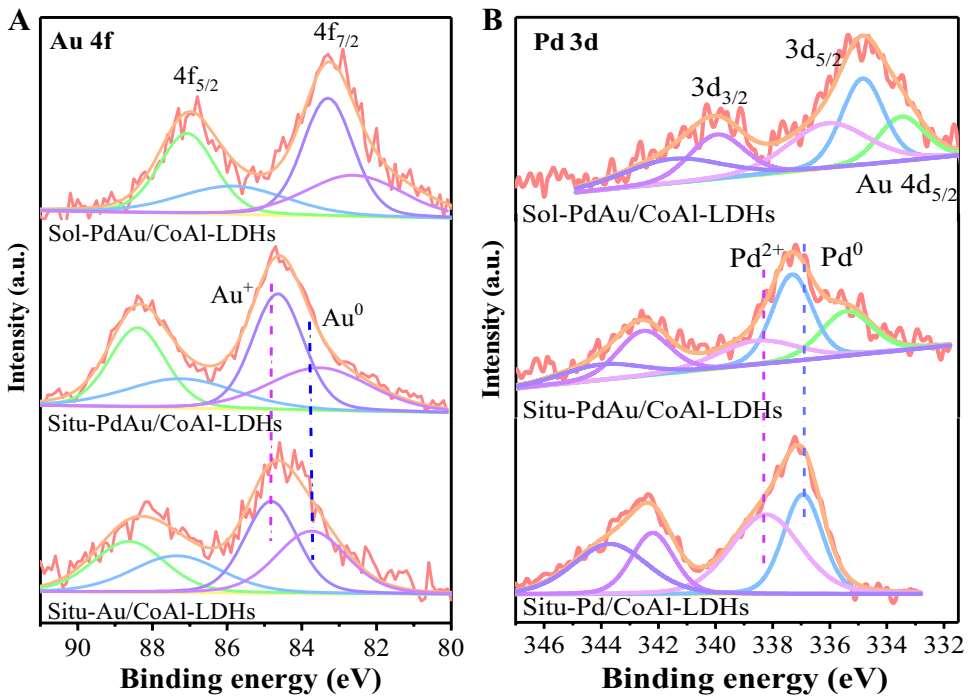

Fig. 5 XPS spectra of **a** Au 4f, **b** Pd 3d over the catalysts

Table 2 Properties of supported catalysts prepared using CoAl-LDHs

Samples	Situ-Au/CoAl-LDH	Situ-Pd/CoAl-LDH	Situ-PdAu/CoAl-LDH	Sol-PdAu/CoAl-LDH
Metal loading (wt. %)[a]				
Pd	–	0.50	0.18	0.18
Au	0.50	–	0.32	0.32
Metal loading (wt. %)[b]				
Pd	–	0.33	0.11	0.17
Au	0.31	–	0.08	0.14
Particle size[c] (nm)	–	–	1.2 ± 0.3	2.9 ± 0.8
Dispersion[c] (%)	–	–	73	31
Pd/Au molar ratio in the bulk[d]	–	–	1.2	1.1
Pd/Au molar ratio in the surface[e]	–	–	0.7	0.5

[a]Theoretical value
[b]Determined by ICP-AES
[c]Based on HRTEM
[d]Determined by STEM
[e]Determined by XPS

that of the previously reported noble metal catalysts, while the high E_a value is obtained over Sol-PdAu/CoAl-LDHs (76.5 kJ mol^{-1}). This result suggests that the characteristics of Situ-PdAu/CoAl-LDHs could lower the barrier of activation for the reaction, and thus improve the activity. Except for activity, selectivity toward benzaldehyde of the catalysts is also displayed in Fig. 6b. At iso-conversion, higher benzaldehyde selectivity are observed over Situ-PdAu/CoAl-LDHs than that over Sol-PdAu/CoAl-LDHs. It is noteworthy that a significant decrease of selectivity (16%) over Sol-PdAu/CoAl-LDHs is captured with the conversion increasing, while the selectivity over the sample prepared by the spontaneous in situ reduction route only demonstrates ca. 6% of decrease. Especially, when the conversion of benzyl alcohol reaches 95%, benzaldehyde selectivity over Situ-PdAu/CoAl-LDHs is up to 94%, much higher than that of Sol-PdAu/CoAl-LDHs and some reports in Table 3 [43–48]. This illustrates that

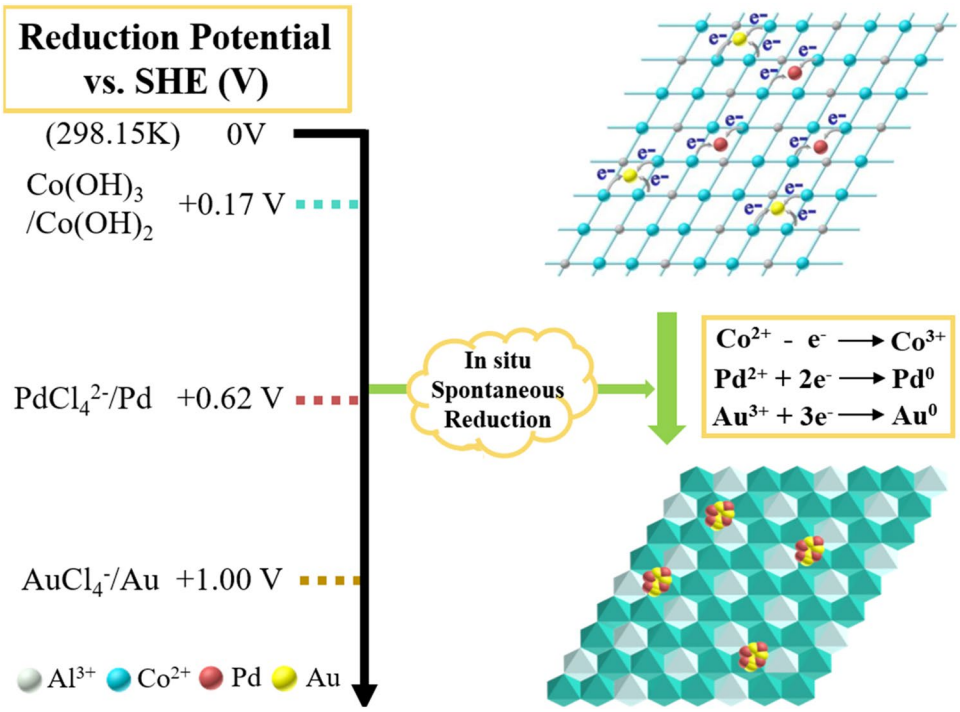

Scheme 1 Schematic illustration of PdAu/CoAl-LDHs prepared by spontaneous in situ redox method

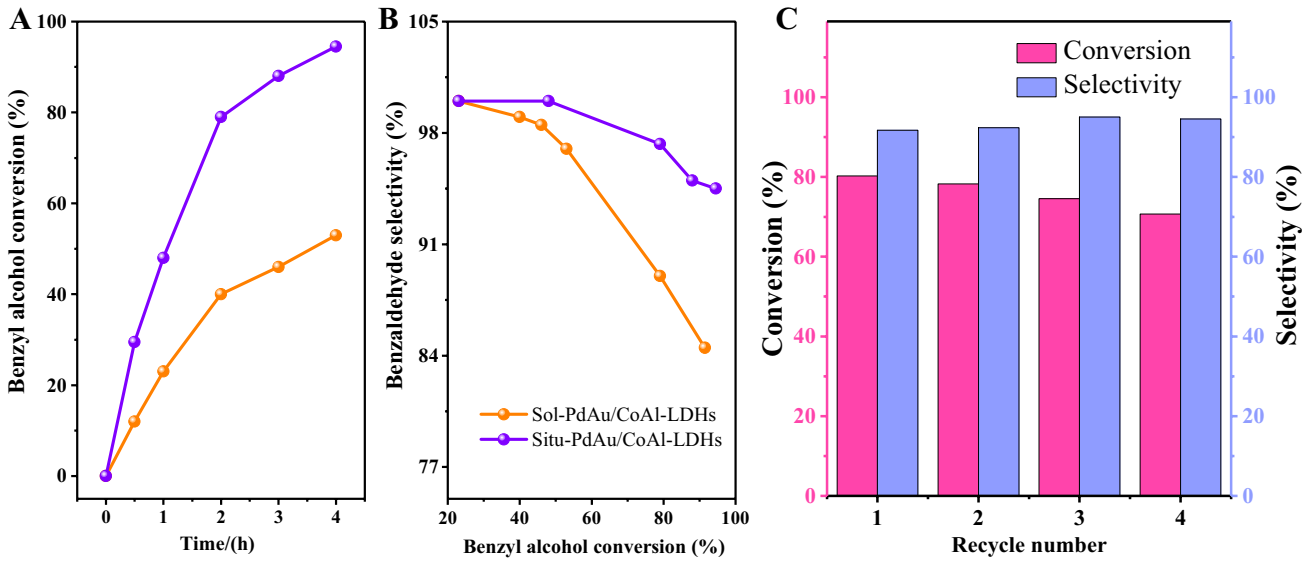

Fig. 6 Plots of **a** benzyl alcohol conversion versus reaction time and **b** benzaldehyde selectivity versus benzyl alcohol conversion over two catalysts, **c** reusability of Situ-PdAu/CoAl-LDH catalyst. Conditions: 5 mL toluene, 3 mL benzyl alcohol, benzyl alcohol: metal = 10,000:1 (molar ratio), 0.1 MPa O_2, 100 °C

PdAu catalyst derived from the spontaneous in situ route is a more selective catalyst, which could be attributed to surface electron starvation of Pd and Au in the Situ-PdAu/CoAl-LDHs confirmed by XPS analysis, promoting the hydroxyl groups react with O_2 to produce benzaldehyde [49, 50]. Furthermore, the recycling experiment was also carried out at 2.5 h corresponding to 80% of conversion to investigate the stability of Situ-PdAu/CoAl-LDHs catalyst (Fig. 6c). The conversion and selectivity fluctuates in a small range, confirming this catalyst keep stable after four cycles.

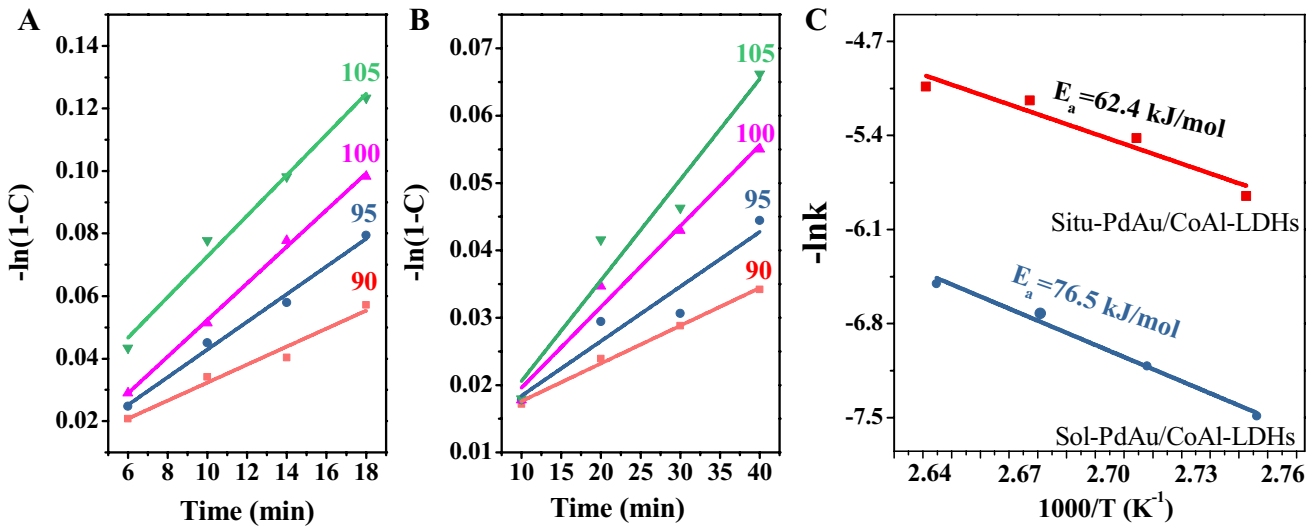

Fig. 7 The plots of $-\ln(1-c)$ versus time over **a** Situ-PdAu/CoAl-LDHs, **b** Sol-PdAu/CoAl-LDHs at different temperatures, **c** Arrhenius plots for oxidation of benzyl alcohol over two catalysts

Table 3 Catalytic behavior of benzaldehyde on various catalysts

Entry	Catalysts	Conv. (%)	Sel. (%)		
			Benzaldehyde	Benzoic acid	Benzyl benzoate
1	Situ-PdAu/CoAl-LDH	95	94	3	3
2	Pd/CN [43]	33	100	–	–
3	Au/TiO_2-400 [44]	90	73	–	–
4	RuO_2/CoAl-LDH [45]	90	99	–	–
5	Pd_1Au_{24}/CNT [46]	74	24	53	23
6	1% (1Au-7Pd) [47]	50	85.8	5.5	6.8
7	Pd/HMDS-S16 [48]	20.3	89.8	0	10.2 (toluene)
8	Pd/APS-S16 [48]	21.0	94.6	0.4	5.0 (toluene)
9	Pd/SiO_2 [48]	22.7	82.9	0	17.1 (toluene)
10	Pd/Al_2O_3 [48]	43.3	64.9	0.2	34.9 (toluene)

4 Conclusion

In this work, Co and Al elements were introduced into the layer to fabricate the reductive CoAl-LDH support. This kind of material was simultaneously employed as support and reducing agent to prepare supported PdAu catalyst by in situ spontaneous reduction method. XPS analysis of Situ-PdAu/CoAl-LDHs catalyst revealed Pd and Au precursors underwent the redox process by the reducing Co site in the support, in which Co^{2+} was oxidized to Co^{3+}, while active metal ions including Au^{3+} and Pd^{2+} were reduced to Au^0 and Pd^0. HRTEM images further confirmed that metallic Pd and Au were successfully reduced by reductive support without the additional reducing regent, and homogeneously distributed on the support with the particle size of 1.2 ± 0.3 nm and the metal dispersion of 73%. However interestingly, the PdAu/CoAl-LDHs catalyst prepared by sol-immobilization method possessed bigger particle size (3.0 ± 0.8 nm) and poor metal dispersion (31%). The selective oxidation of benzyl alcohol was employed as probe reaction to test the catalytic behavior over the synthesized Situ-PdAu/CoAl-LDHs and Sol-PdAu/CoAl-LDHs catalysts. As for intrinsic activity, Situ-PdAu/CoAl-LDHs catalyst exhibited a Ea of 62.4 kJ mol^{-1}, 22% lower than that of Sol-PdAu/CoAl-LDHs (76.5 kJ mol^{-1}). When the reaction time reached to 4 h, the conversion of benzyl alcohol over Situ-PdAu/CoAl-LDHs was 95% and benzaldehyde selectivity still maintained at 94%. Small size of PdAu nanoparticles facilitated the exposure of more active sites for the adsorption and activation of benzyl alcohol, and thus improved the activity. Preferable selectivity was ascribed to the surface electron starvation of active metals that promoted the hydroxyl groups reacting with O_2 to produce benzaldehyde.

Acknowledgements This work was supported by the National Natural Science Foundations of China (21706009, 21627813, 21908002), China Postdoctoral Science Foundation (2019M660416, 2020T130045), the Fundamental Research Funds for the Central Universities (buctrc201921) and PetroChian Science and Technology Management Department (2016E-0703).

Compliance with Ethical Standards

Conflict of Interest The authors declare that they have no conflict of interest.

References

1. Wu G, Zheng X, Cui P et al (2019) Nat Commun 10:4855
2. Hunt ST, Milina M, Alba-Rubio AC et al (2016) Science 352:974–978
3. Wei S, Li A, Liu JC et al (2018) Nat Nanotech 13:856–861
4. Farmer JA, Campbell CT (2010) Science 329:933–936
5. Chong S, Zhang G, Zhang N et al (2016) Ultrason Sonochem 32:231–240
6. Zhang N, Zhang G, Chong S et al (2018) J Environ Manage 205:134–141
7. Iqbal S, Kondrat SA, Jones DR et al (2015) ACS Catal 5:5047–5059
8. White RJ, Luque R, Budarin VL et al (2009) Chem Soc Rev 38:481–494
9. Astruc D, Lu F, Aranzaes JR (2005) Angew Chem Int Ed 44:7852–7872
10. Li XN, Yuan Z, He SG (2014) J Am Chem Soc 136:3617–3623
11. Li ZY, Yuan Z, Li XN et al (2014) J Am Chem Soc 136:14307–14313
12. Cargnello M, Doan-Nguyen VV, Gordon TR et al (2013) Science 341:771–773
13. Choi HC, Shim M, Bangsaruntip S et al (2013) J Am Chem Soc 124:9058–9059
14. Qi H, Yu P, Wang Y et al (2015) J Am Chem Soc 137:5260–5263
15. Sotiles AR, Baika LM, Grassi MT et al (2018) J Am Chem Soc 141:531–540
16. Wang Q, O'Hare D (2012) Chem Rev 112:4124–4155
17. Sideris PJ, Nielsen UG, Gan Z et al (2008) Science 321:113–117
18. Rives V, Arco M, Martín C (2013) J Controlled Release 169:28–39
19. Meng X, Yang Y, Chen L et al (2019) ACS Catal 9:4226–4235
20. Li H, Yang T, Jiang Y et al (2020) J Catal 385:313–323
21. Mekasuwandumrong O, Somboonthanakij S, Praserthdam P et al (2009) Ind Eng Chem Res 48:2819–2825
22. Mishra G, Dash B, Pandey S (2018) Appl Clay Sci 153:172–186
23. Chen X, Wu G, Chen J et al (2011) J Am Chem Soc 133:3693–3695
24. Zhang F, Zhao X, Feng C et al (2011) ACS Catal 1:232–237
25. Liu X, Zhou A, Pan T et al (2016) J Mater Chem A 4:8421–8427
26. Zhuo K, Wang J, Zhang Q et al (1999) Carbohyd Res 316:26–33
27. Jacob KT, Saji VS, Reddy SNS (2007) J Chem Thermodyn 39:230–235
28. Feng J, He Y, Liu Y et al (2015) Chem Soc Rev 44:5291–5319
29. Fan G, Li F, Evans DC et al (2014) Chem Soc Rev 43:7040–7066
30. Cardenas-Lizana F, Hao Y, Crespo-Quesada M et al (2013) ACS Catal 3:1386–1396
31. Lear T, Marshall R, Lopez-Sanchez J et al (2005) J Chem Phy 123:174706
32. Han F, Xia J, Zhang X et al (2019) RSC Adv 9:17812–17823
33. Li Z, Wang R, Xue J et al (2019) J Am Chem Soc 141:17610–17616
34. Liu ZQ, Cheng H, Li N et al (2016) Adv Mater 28:3777–3784
35. Ma TY, Dai S, Jaroniec M et al (2014) J Am Chem Soc 136:13925–13931
36. Chaudhari K, Xavier PL, Pradeep T (2011) ACS Nano 5:8816–8827
37. Zhao S, Li K, Jiang S et al (2016) Appl Catal B 181:236–248
38. Shi Y, Yang H, Zhao X et al (2012) Catal Commun 18:142–146
39. Chen J, Yan D, Xu Z et al (2018) Environ Sci Technol 52:4728–4737
40. Liu H, Zakhtser A, Naitabdi A et al (2019) ACS Catal 9:10212–10225
41. Yang P, Pan J, Liu Y et al (2018) ACS Catal 9:188–199
42. Liu Y, McCue AJ, Yang P et al (2019) Chem Sci 10:3556–3566
43. Xu J, Shang J, Chen Y (2017) Appl Catal A 542:380–388
44. Lavenn C, Demessence A, Tuel A (2015) J Catal 322:130–138
45. Zhang N, Du Y, Yin M (2016) RSC Adv 6:49588–49596
46. Xie S, Tsunoyama H, Kurashige W (2012) ACS Catal 2:1519–1523
47. Pritchard J, Kesavan L, Piccinini M et al (2010) Langmuir 26:16568–16577
48. Chen Y, Lim H, Tang Q (2010) Appl Catal A 380:55–65
49. Conte M, Miyamura H, Kobayashi S (2009) J Am Chem Soc 131:7189–7196
50. Feng J, Ma C, Miedziak PJ et al (2013) Dalton Trans 42:14498–14508

Affiliations

Shuai Chen[1] · Haiping Li[1] · Yanan Liu[1,2] · Junting Feng[1,2] · Yufei He[1,2] · Yanfei Wang[3] · Dianqing Li[1,2]

✉ Yanan Liu
ynliu@mail.buct.edu.cn

✉ Yufei He
yfhe@mail.buct.edu.cn

[1] State Key Laboratory of Chemical Engineering, Beijing University of Chemical Technology, Beijing 100029, China

[2] Beijing Engineering Center for Hierarchical Catalysts, Beijing University of Chemical Technology, Beijing 100029, China

[3] Petrochina Petrochemical Research Institute, Beijing 102206, China